Development of 4D printed intravesical drug delivery systems: scale-up of film coating

Marco Uboldi[1], Andrea Gelain[2], Giuseppe Buratti[2], Andrea Gazzaniga[1], Alice Melocchi[1]*, Lucia Zema[1]

[1]Sezione di Tecnologia e Legislazione Farmaceutiche "Maria Edvige Sangalli", Dipartimento di Scienze Farmaceutiche, Università degli Studi di Milano, via Giuseppe Colombo 71, 20133, Milano, Italy;

[2]Freund-Vector Corporation European Lab, via E. Mattei, 2, 20852 Villasanta (MB), Italy.

*Corresponding author: alice.melocchi@unimi.it; +39 0250324665

Keywords: 3D printing; fused deposition modeling; film-coating; controlled release; retentive systems; shape memory effect.

Abstract

The potential of 4D printing in the development of coated expandable drug delivery systems (DDSs) targeting long-lasting retention and controlled release of drugs into hollow muscular organ has recently been investigated. In this respect, the shape memory behavior of a pharmaceutical-grade poly(vinyl alcohol) (PVA) turned out effective for attaining prototypes capable to be programmed in a temporary configuration suitable for administration, and to recover the original encumbered shape ensuring retention at the target site. Moreover, the shape memory effect was shown independent of the presence of insoluble but permeable coatings. Based on the encouraging results collected so far at the lab-scale using a home-made equipment, in this work the industrial scale-up of the coating process was approached in collaboration with a company leader in the manufacturing of pharmaceutical machinery. Dealing with reservoir-like expandable prototypes suitable for intravesical applications, a dedicated coating process was set-up using an Eudragit® NE-based formulation. Samples provided with different original and temporary shapes, printed structures and fillings of the inner cavities were considered as substrates. The robustness of the process was demonstrated checking the coated prototypes in terms of physical-technological properties, shape memory effect and release performance in urine simulated fluids.

1. Introduction

Recently, a pharmaceutical-grade poly(vinyl alcohol) (PVA) was proved suitable for the development of expandable drug delivery systems (DDSs) intended for long-lasting maintenance and controlled release into hollow muscular organs such as the bladder and the stomach [1-3]. With respect to more traditional strategies towards organ-retention, entailing high-density, low-density, magnetic and mucoadhesive dosage forms as well as devices undergoing expansion upon either swelling or elastic deployment, the systems proposed are able to increase their encumbrance thanks to the water-induced shape memory behavior PVA is provided with [4-7]. Indeed, the metastable temporary configuration PVA-based prototypes were forced to take on was spontaneously reversed to the original shape attained during manufacturing by hot-processing techniques. This predictable shape evolution was triggered by simple contact with aqueous fluids at body temperature and occurred over a certain period of time. As a result, for specimens manufactured by fused deposition modeling (FDM) 3D printing, the time itself could be identified as their 4^{th} dimension. In this respect, the systems proposed represented one of the first attempts towards 4D printing in the drug delivery field for the production of smart DDSs.

Based on the hollow muscular organ targeted, specific therapeutic goals could be pursued by making use of different expandable DDSs relying on the above described shape memory effect [11,12]. Starting from different PVA-based formulations, prototypes with various temporary shapes (*e.g.* supercoiled helices, I- and paper clip shapes) were obtained, having overall dimension compatible with the selected administration route. On the other hand, the original shapes to be recovered *in situ* (*e.g.* U- and atom-like shapes, conical and cylindrical helices) were designed so as each system could gain enough spatial encumbrance to ensure its retention in the target organ, without obstructing relevant orifices or damaging the internal walls.

First, matrix-like prototypes, in which a drug tracer was embedded into the main polymeric component, pointed out the desired shape memory behavior, irrespective of their original/temporary shape as well as of the process employed for their manufacturing. These matrices were characterized

by a prolonged release of the active ingredient conveyed, the rate of which was consistent with the molecular weight of the selected PVA. Preliminary studies carried out on specimens coated with insoluble films based on methacrylic copolymers were successful in highlighting the possibility to modulate the rate of release and improve the mechanical properties [Uboldi et al., 2022b]. Moreover, in order to further increase the versatility of the DDSs, inner cavities were designed, specifically developed to be extemporaneously filled with different drugs/formulations [Uboldi et al., 2023]. Finally, biocompatibility was preliminarily assessed by evaluating cell viability and inflammatory response after exposure to uncoated and coated samples based on the different PVAs employed.

As the data collected so far were promising, the aim of the present work was to start the industrial scale-up of the expandable DDSs under investigation. In particular, the coating process, which was deemed strategic for the performance of the systems and was previously carried out at a lab-scale by means of an in-house assembled equipment, needed to be improved [13]. This was especially challenging because of the configuration and dimensions of the retentive prototypes, the shape transformation they must undergo and the properties they have to maintain, *i.e.* the shape memory effect. Therefore, in collaboration with a global full service company specialized in pharmaceutical machinery (*i.e.* Freund-Vector Corporation), a dedicated process was developed in a pilot-scale equipment. Prototypes suitable for intravesical administration, having different original and temporary shapes, printed structures (*i.e.* infill) and inner cavities filled with various formulations were considered as substrates for this work, willing to challenge the process and determine its potential towards industrial-scale coating of 4D printed expandable DDSs.

2. Materials and Methods

2.1 Materials

PVA (Gohsenol™ EG 05P Mitsubishi Chemical, J); glycerol (Pharmagel, I; GLY); acetaminophen for direct compression (Rhodia, I; AAP); calcium phosphate (Emcompress®, JRS, D); microcrystalline cellulose (Avicel-PH 200, IFF, I); soy polysaccharides (Emcosoy®, JRS, D)

magnesium stearate (A.C.E.F., I); talc (A.C.E.F., I); colloidal silica (A.C.E.F., I); low-viscosity hydroxypropyl methylcellulose (Methocel™ E5, Colorcon, I; HPMC E5); high-viscosity hydroxypropyl methylcelluloses (Methocel™ K100M and Methocel™ K200M, Colorcon, I; HPMC K100M and HPMC K200M); tween 80 (Vitipure, Clariant, I); ready-to-use dispersion of methacrylic acid copolymers (Eudragit® NE 30D, Evonik, D).

2.2. Methods

2.2.1 3D Printing

After being kept in an oven at 40 °C for 24 h, PVA powder was mixed in a mortar with GLY, which was added dropwise. The resulting mixture was oven dried (40 °C for 8 h) and then grounded by means of a blade mill. The < 250 μm fraction was collected and used for the production of filaments [14]. The latter was loaded into a twin-screw extruder (Haake™ MiniLab II, Thermo Scientific, US-WI) equipped with counter-rotating screws and a custom-made aluminum circular die (ø = 1.80 mm). Process temperature and screw speed were set at 175 °C and at 100 rpm, leading to a maximum torque of about 100 N·cm. Extruded rods were manually pulled through a caliper connected to the extruder and set at 1.80 mm to calibrate the relevant diameter and increase the yield of filaments suitable for 3D printing (*i.e.* diameter of 1.75 ± 0.05 mm). After cooling, filament diameter was further verified every 5 cm, and portions out of specifications were eliminated. Starting from those PVA-based filaments, 3D printing of prototypes was carried out using a Kloner3D 240® Twin printer (Kloner3D, I) equipped with 0.5 mm nozzle (Table 1).

Table 1: printing parameters

Printing temperature	200 °C
Build plate temperature	50 °C
Infill percentage	100% or 50%
Infill pattern	rectilinear
Layer height	0.10 mm
Number of perimeters	2
Number of top/bottom layers	2
Printing speed	23 mm/s

Computer-aided design (CAD) files were purposely developed for the fabrication of I- and U-shaped samples having inner reservoirs for drug filling (Figure 1). Items were designed using Autodesk® Autocad® 2016 software version 14.0 (Autodesk Inc., US-CA), saved in .stl format and imported to the 3D printer software (Simplify 3D, I). The printing process was interrupted at the 25th layer to manual fill the sample cavities with:

- AAP powder;
- AAP powder formulations containing either HPMC K100M or HPMC K200M (10:90 *ratio* by weight);
- 8 mini-tablets (4 for each cavity, placed horizontally) prepared from the AAP powder formulations reported in Table 2a.

The process was then restarted having the nozzle completing just the walls of the cavities (*i.e.* going around the filling formulation without touching them) for the remaining 1 mm in height. Only when the walls were completed, the cavities were closed with the desired top layers. Indeed, the nozzle moved above the filled area and layered the molten material from one cavity wall to the other (which worked as anchoring points thus ensuring complete closure of the samples.

By way of example, photographs of U-shaped samples during relevant 3D printing and filling are reported in Figure 2.

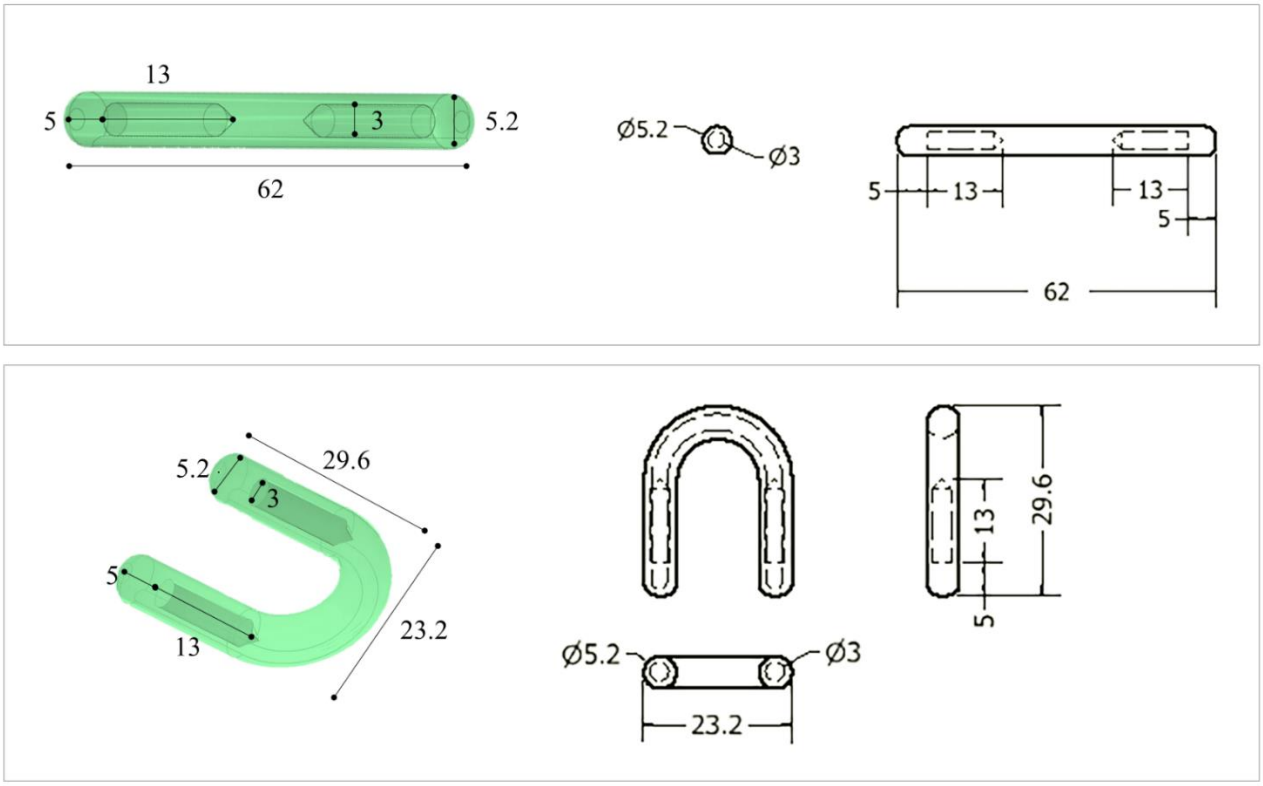

Figure 1: electronic models of I- and U-shaped samples with dimensional details (in mm) and relevant 2D sections

Table 2: composition of the formulations used for the preparation of tablets having either a) 2.5 or b) 10 mm diameter

a	**Composition (w/w %)**	
AAP	10	10
HPMC K100M	87.8	/
HPMC K200M	/	87.8
Magnesium stearate	2	2
Colloidal silica	0.2	0.2

b	**Composition (w/w %)**
AAP	20
Calcium phosphate	32.40
Microcrystalline cellulose	32.40
Talc	10
Soy saccharides	3
Magnesium stearate	2
Colloidal silica	0.2

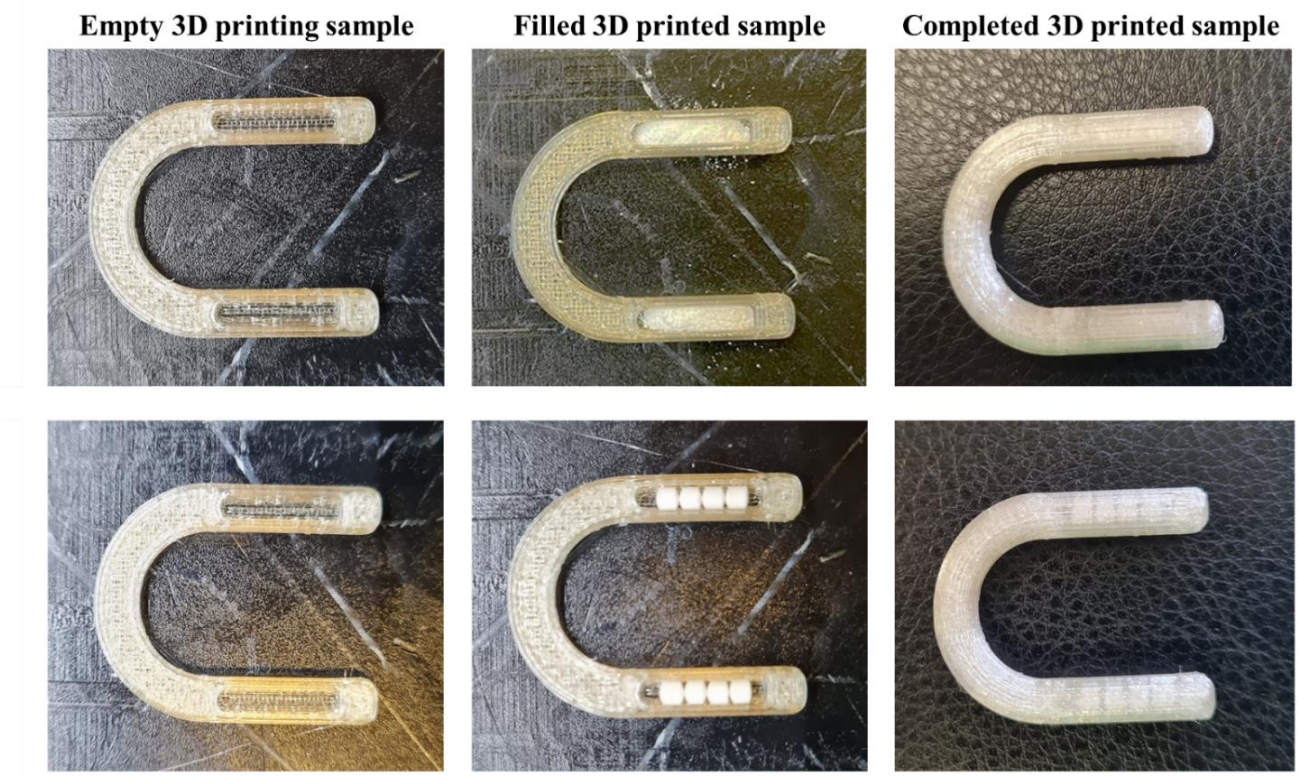

Figure 2: photographs of U-shaped samples (100% infill) during relevant printing and filling with either (top) HPMC K100M-based powder formulation or (bottom) relevant mini-tablets

Mini-tablets were manufactured by direct compression using a tableting machine equipped with convex punches of 2.5 mm in diameter (AM-8S, Officine Ronchi, I). The components previously weighted (Gibertini, I) were mixed in a 2.5 kg rotary body mixer (30° arm inclination, 25 rpm for 15 min; Cyclops, VIMA, I). After 12 min, magnesium stearate was added to the blend and the mixing process was restarted for 3 min. The machine was set (compression force, $F_a \approx 9/10$ kN) to obtain tablets with a reproducible weight of 25 ± 1.25 mg and characterized by a crushing strength around 20 N. Tablets to be employed as substrates for the coating process were also prepared (Table 2b), using the same machinery above-described but equipped with convex cup punches of 10 mm in diameter. F_a was set to ≈ 97/110 kN to obtain tablets with a reproducible weight of 570 mg ± 4% and characterized by a crushing strength around 25 N.

2.2.2 Coating

Tablet cores and printed prototypes were coated using a 30% (w/v) aqueous suspension of Eudragit® NE 30D, prepared as reported in Table 3 [15]. HPMC was first dissolved in one third of water, kept at 50 °C under continuous stirring. Once a clear solution was formed, the rest of water (maintained at room temperature) was added to the solution together with talc and tween 80, mixing the suspension for at least 10 min. The latter was then poured in the Eudragit® NE 30D liquid formulation and the mixing was continued for 5 min. Before use, the resulting mixture was passed through a 0.5 mm sieve. The process was carried out in a modified LDCS Hi-Coater® (Freund-Vector; Milan, I). Description of the coating process developed is the main topic of the Results and discussion section.

Table 3: composition of the coating formulation

	Amount (w/w %)
Eudragit® NE 30D	30
Talc	10
HPMC E5	1
Tween 80	3
Distilled water	56

2.2.3 Characterization

DSC analyses were performed on printed prototypes by a DSC Q100 TA Instruments equipment (US-DE), using nitrogen as a purge gas (70 mL/min). Indium was used as a calibration standard. Samples of about 10 mg were heated in aluminum pans from -50 °C to 240 °C, maintained at this temperature for 1 min, cooled down to -50 °C and reheated up to 240 °C. Both the heating and cooling steps were run at 10 °C/min. Resulting thermograms were used to identify the glass transition temperature (T_g) of the material, so as to set the conditions of the shape memory test, as reported below (resulting T_g of PVA-based specimens ≈ 20 °C).

While all the specimens were characterized for weight (n = 6; Analytical balance, Gibertini, I), thickness of the coating layer was determined on the coated samples (n = 6) and the relevant weight gain (w_g) was calculated. For measuring the thickness of the coating layer, photographs of the cross-sections of purposely-cut samples were acquired, using a digital microscope (Digital Microscope AM-413T, Dino-Lite, I; resolution = 1.3 Megapixel - 1280 x 1024), and processed by a dedicated software (ImageJ, US-MD). Coated tablets were centrally cut (*i.e.* in a single position) by means of a manual tablet splitter (P.B. Pharma, I) and thickness measurements were collected either on their faces (6 points) or on the centre band (4 points) (Figure 3). On the other hand, printed specimens were manually cut in 6 positions (1-6, Figure 3) by means of a scalpel, as before described [16]. This way, thickness of the coating layer was determined both on the length (*i.e.* 1-4 positions) and on the ends (*i.e.* 5-6 positions) of the samples. On each photograph, at least 6 different measurements were taken. Before collecting any data, all the specimens were checked with an optical microscope (100-100x, Zetalab, I), in order to verify that the cutting step did not cause major damages neither to the film nor to the prototype itself.

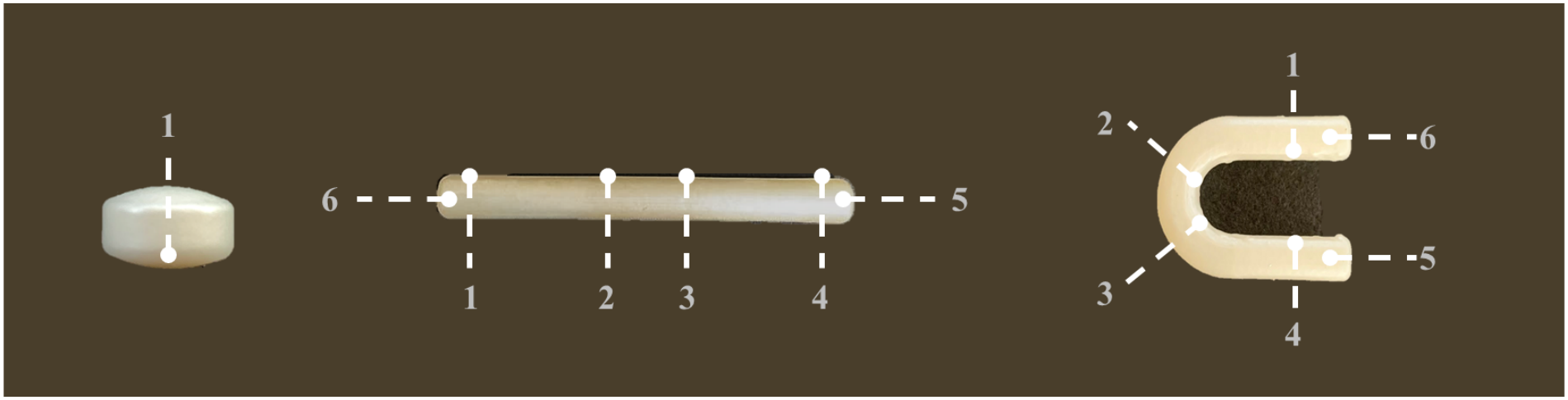

Figure 3: outline of the positions in which the different specimens were cut for measuring the coating thickness

The shape memory test was carried out on I- and U-shaped samples as before described, entailing first programming of the temporary shape and then recovery of the original one [1]. More into detail, the programming step involved heating of the samples up to 55 °C (*i.e.* 35 °C above the T_g measured *via* DSC). By means of specially designed tools, the specimens, maintained at 55 °C, were programmed to take on the desired temporary shape. Samples having original U-shape were deformed to take on a temporary I-shape, and *viceversa*. As the specimens needed to be maintained at least 20 °C below their T_g to avoid early recovery of the original shape, they were cooled in the fixed temporary shape at -20° C until testing (at least for 8 h). Recovery of the original shape was triggered upon exposure of the samples in their temporary shape to temperatures overcoming their T_g. Therefore, they were immersed into 100 mL of unstirred simulated urine, prepared as reported by Sherif and coworkers, kept at 37 ± 0.5 °C by using a thermoregulated bath [17]. The recovery process was monitored using a digital camera positioned at 10 cm above the samples (n = 3, GoPro Hero Session, US-CA). The photographs collected were processed by means of a specific software (ImageJ, US-MD) to measure the variation of the angle between the two arms (α) of the samples occurring during the recovery. Recovery index (RI) versus time curves were then built, with RI calculated as follows:

- for specimens having original I-shape

$$RI = \frac{\alpha - \alpha_p}{\pi - \alpha_p} \qquad \text{Eq. (1)}$$

- for specimens having original U-shape

$$RI = 1 - \frac{\alpha}{\alpha_p} \qquad \text{Eq. (2)}$$

where α_p is the angle obtained in the programming phase (angles in rad). Moreover, the time the samples needed to recover 50 and 80% of their original shapes (*i.e.* $t_{RI50\%}$ and $t_{RI80\%}$) were determined. A simple outline of the shape recovery experiments performed is reported in Figure 4, also highlighting the angles used for the calculation of the RI.

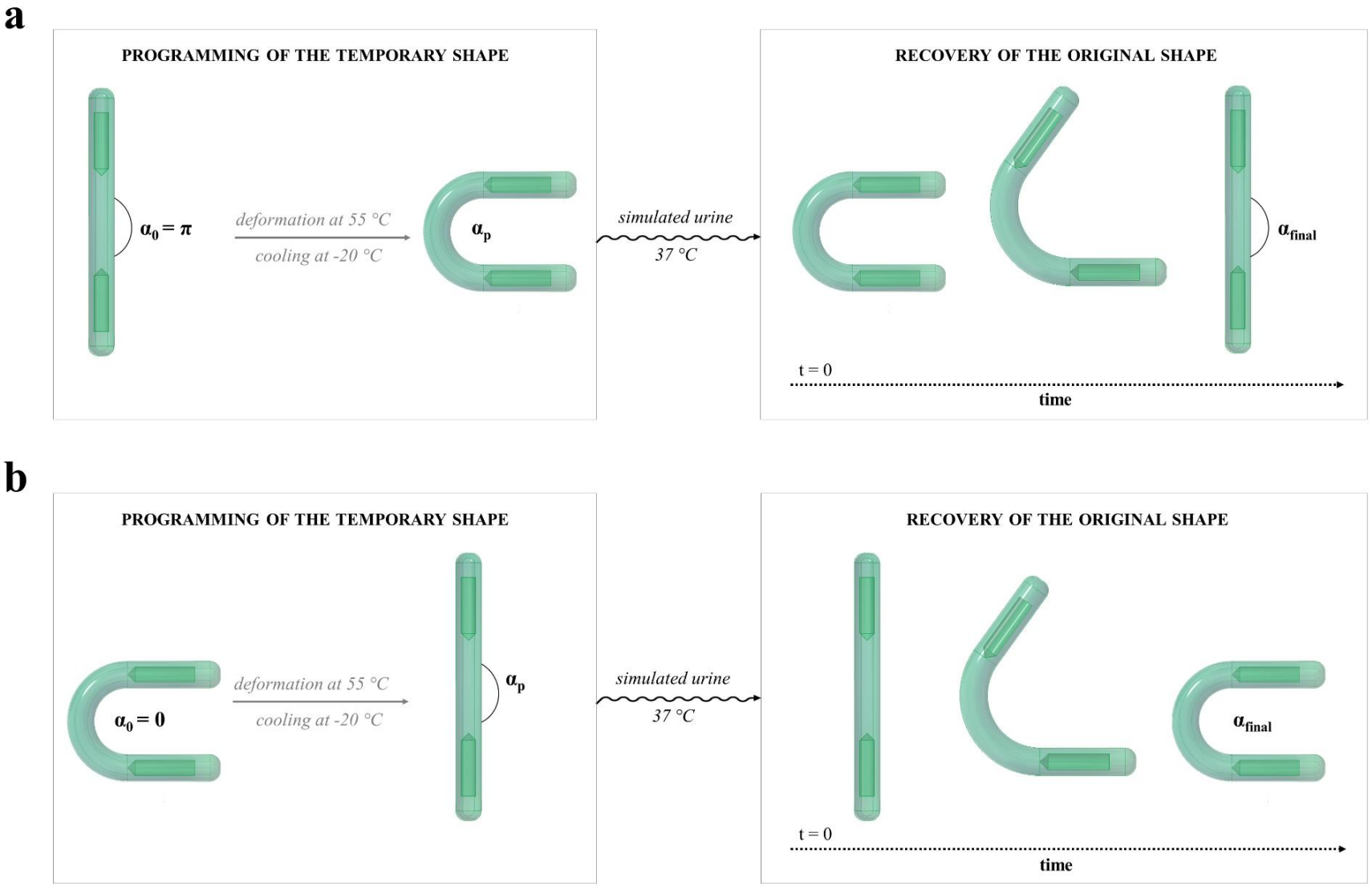

Figure 4: outline of the shape recovery experiment performed on samples with original a) I and b) U shape and the angles used to define relevant RI

Uncoated and coated specimens (*i.e.* tablets and printed prototypes) were tested for release using a USP38 dissolution apparatus 2 (10 rpm, 37 ± 0.5 °C; Distek, CH; n = 3). 400 mL of simulated urine were used as the dissolution medium. Fluid samples were withdrawn at specific time points and assayed spectrophotometrically (λ = 248 nm). By linear interpolation of the release data immediately before and after the time point of interest, times to 10% and 90% release (*i.e.* $t_{10\%}$ and $t_{90\%}$, respectively) were calculated, using $t_{10\%}$ to define the lag phase [18].

3. Results and discussion

3.1 Coating process

Expandable 4D printed DDSs intended for retention into hollow organs are characterized by cumbersome complex original shapes. The latter should not only be modified to suitable temporary shapes enabling administration, but also recovered upon contact with aqueous fluids at body temperature, as they are responsible for the system performance into the target area over time. In this respect, when expandable DDSs are coated, the characteristics of the film applied are expected to impact on release of the conveyed drug, on programming of the temporary shape and on recovery of the original one. Therefore, the possibility of achieving uniform and continuous films of reproducible thickness over the entire surface of specimens having different geometry, weight and apparent density, with a controllable and scalable industrial process was addressed. The topic was deemed particularly interesting as the scale-up of film-coating processes has already been identified as challenging using conventional substrates, such as tablets provided with pseudo-spherical shapes [19].

Process and equipment set-up were carried out in collaboration with Freund-Vector, giving the experience of the Company in developing new machines intended for the pharmaceutical industry and in modifying already existing ones based on the process to be implemented. More into detail, a R&D coating equipment characterized by a perforated pan of 4 L capacity and a 3-ways nozzle (*i.e.*

control, atomizer and pattern) of 0.8 mm in diameter was employed. This coating pan was selected because, although compatible with lab and pilot scale, it might enable a relatively easy scale-up of the process at the industrial level. I- and U-shaped prototypes with the same surface area were designed and successfully printed. They were provided with inner cavities, filled with different formulations, and had diverse weight/apparent density as a consequence of infill percentage set during 3D printing (*i.e.* 50 and 100% infill). Based on the experience previously gained, the prototypes were designed with a pseudo-circular cross-section, rounded ends, thus avoiding the presence of sharp angles in view of the intended application, and a flat bottom surface, which was deemed strategic for the adhesion of the first layers during FDM printing (Figure 1). Both I and U were selected as screening shapes because the resulting specimens were characterized by peculiar difficulties in moving inside the pan and in being exposed to the sprayed formulation. Indeed, I-shaped samples mainly rolled on their major direction without flipping on the shortest one, while those having U-shape showed a tendency to engage between each other. Moreover, the internal curvature area of the U-shaped samples resulted critical in terms of frequency of wetting. To overcome such limitations, the standard deflectors (20 mm in height) mounted in the perforated pan were substituted with purposely built higher ones of 28 mm in height. The latter turned out more effective in breaking the flow and allowed easier overturn of samples during relevant rolling, increasing the chances of exposing their entire surface to the spray cone. However, the geometry of both I- and U-shaped specimens remained critical with respect to the overall pan capacity and the addition of tablets (ranging from 500 g to 2.5 kg) was deemed necessary to achieve a pan filling level compatible with its proper functioning. Indeed, being characterized by a pseudo-spherical shape and a smooth surface, the tablets were expected to help the movement of the printed samples, thus having them effectively dragged without engaging or sticking together. In this respect, acceptable results were attained when printed specimens represented 5% in weight of the entire pan filling.

Preliminary coating trials were carried out to fine-tune the process parameters and the selected ones are reported in Table 4. The temperature of the cores during the process was maintained at 28 ± 2 °C.

In addition, the so-called jog mode (also identified as second speed), which would enable slower rotation of the pan during initial heating as well as final cooling phases, was implemented to reduce possible core mechanical stress.

Table 4: selected coating parameters

Inlet air temperaure (°C)	35
Outlet air temperaure (°C)	25
Airflow (m/h)	95
First speed of pan rotation (rpm)	10
Second speed of pan rotation (rpm)	5
Second speed duration (s)	10
Atomizer pressure (bar)	0.01
Pattern pressure (bar)	0.01
Pump rotation speed (rpm)	5

Based on the experience already gained on lab-scale coating of printed prototypes with Eudragit® NE, the process was stopped at pre-determined sampling points, *i.e.* after spraying 250, 500 and 650 g of the coating formulation [20]. Therefore, prototypes having in principle diverse w_g and thickness of the applied film were collected.

All the coated products underwent a curing process (*i.e.* 2 h in a ventilated oven set at 40 °C), which turned out essential to attain a continuous and smooth film (Figure 5). If the cores are characterized by good wettability and are equally exposed to the spraying cone, the amount of the dispersion applied onto them might primarily depend on their surface area. Moreover, a constant thickness increase when greater amounts of the coating formulation were sprayed should indicate a good efficiency of the process, which proceeded without major loss of material. Accordingly, w_g and thickness trends relevant to printed specimens turned out very similar, regardless of their original shape (Figure 6). Dealing with samples with diverse infill so as with different weight, only a limited reduction in the

above mentioned parameters was observed. This was deemed particularly promising especially because changing the mass of the sample might affect its random movement into the coating pan, which is mainly determined by the gravity force. As a result, decreasing the prototype infill percentage could limit the chances of exposure of its various surfaces to the spray cone, with possible impact on w_g, thickness of the resulting film and relevant consistency. In order to assess the quality of the coating process and that of the applied film, the tablets added to the printed specimens under processing were used as the reference product. As expected, focusing on data referring to the same amount of Eudragit® NE dispersion, the increase in weight and thickness of coated tablets was consistent with their reduced surface area with respect to printed items.

Notably, the intra-tablet variability in coating thickness is generally defined as the relative standard deviation and was shown to be dependent on how relevant measurements were taken [21,22]. In this respect, the more spherical the geometry of the cores to be processed, the more uniform the coating is likely to be. Here, CV values relevant to the film thickness of coated samples, either referring to tablets or to the more challenging printed specimens, never exceeded 12% that, in view of data previously published and focused on traditional substrates, were deemed representative of an acceptable process [23]. Indeed, dealing with coating process having rounded tablets as substrate, resulting CVs were reported to be approximately in the 3–6.5% and 4–11% range on the tablet faces and centre bands, respectively. Moreover, according to the literature, the variation in coating thickness between surfaces and centre bands of tablets would strongly depend on the core shape, with round tablets showing the highest reproducibility. Based on these considerations, thickness measurements were collected on different points. Indeed, multiple measurements were taken on each section, with intra-sample variability being in any case comparable to the inter-sample variability in terms of resulting CVs. Focusing on the thickness data relevant to coated tablets, a tendency towards higher CVs on their centre bands was highlighted. Besides being simply associated with a limited reproducibility, such data could also result from a lower amount of coating applied onto this area (Table 5a). Indeed, the centre bands were less likely to be exposed to the spray zone and, even during

such an exposure, the sprayed formulation might be mainly applied to a part of the latter rather than to the whole surface. The same phenomenon could also justify the lower coating thickness registered onto the ends of printed specimens, which were probably characterized by the same difficulty in terms of lateral exposure (Table 5c). Indeed, the chances of the end faces of the specimens to be frontally exposed to the spraying cone during relevant rolling might be very small. On the other hand, thickness data taken along the circumference of the cross-sections of the central portion of both I- and U- shaped items (*i.e.* 1-4 positions) pointed out a limited variability. These findings were overall judged very promising, demonstrating that adequate rolling of the printed specimens was achieved in the coating pan, independent of relevant geometry and apparent density, even enabling the inner area of the U curvature to be coated.

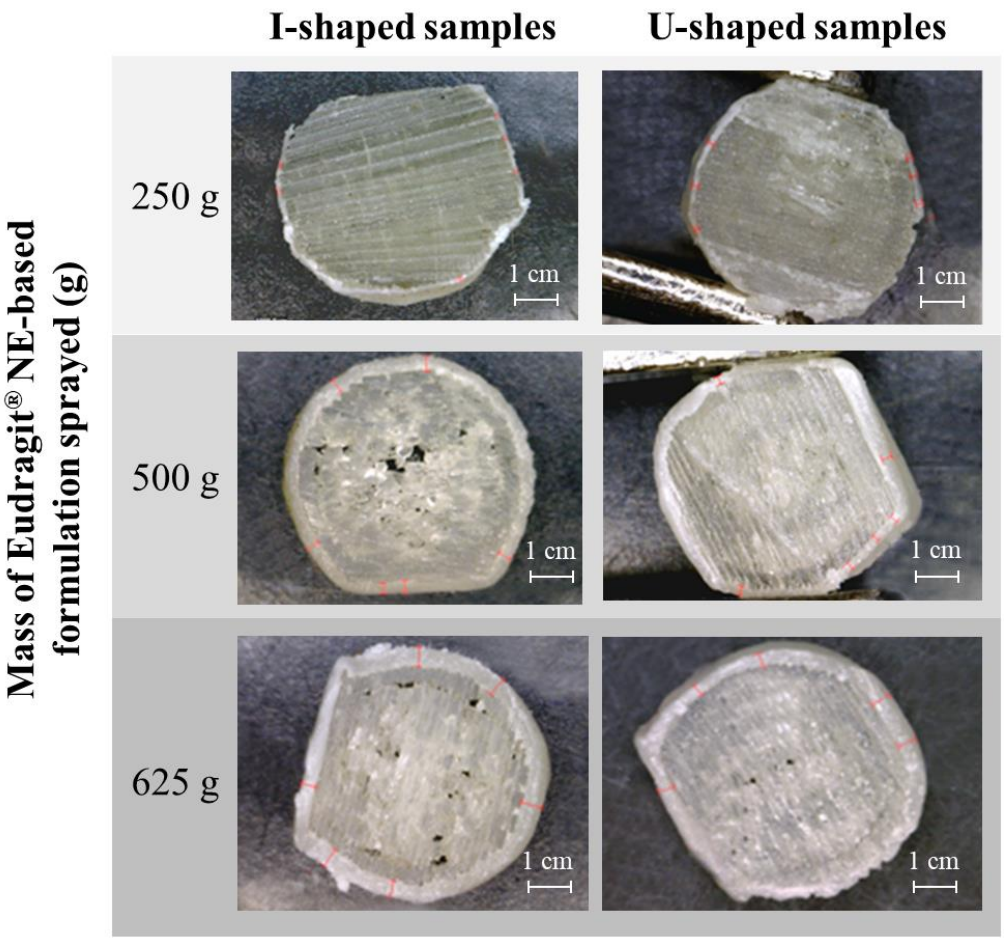

Figure 5: photographs of the cross-sections of I- and U-shaped samples coated with increasing amounts of the Eudragit® NE-based dispersion

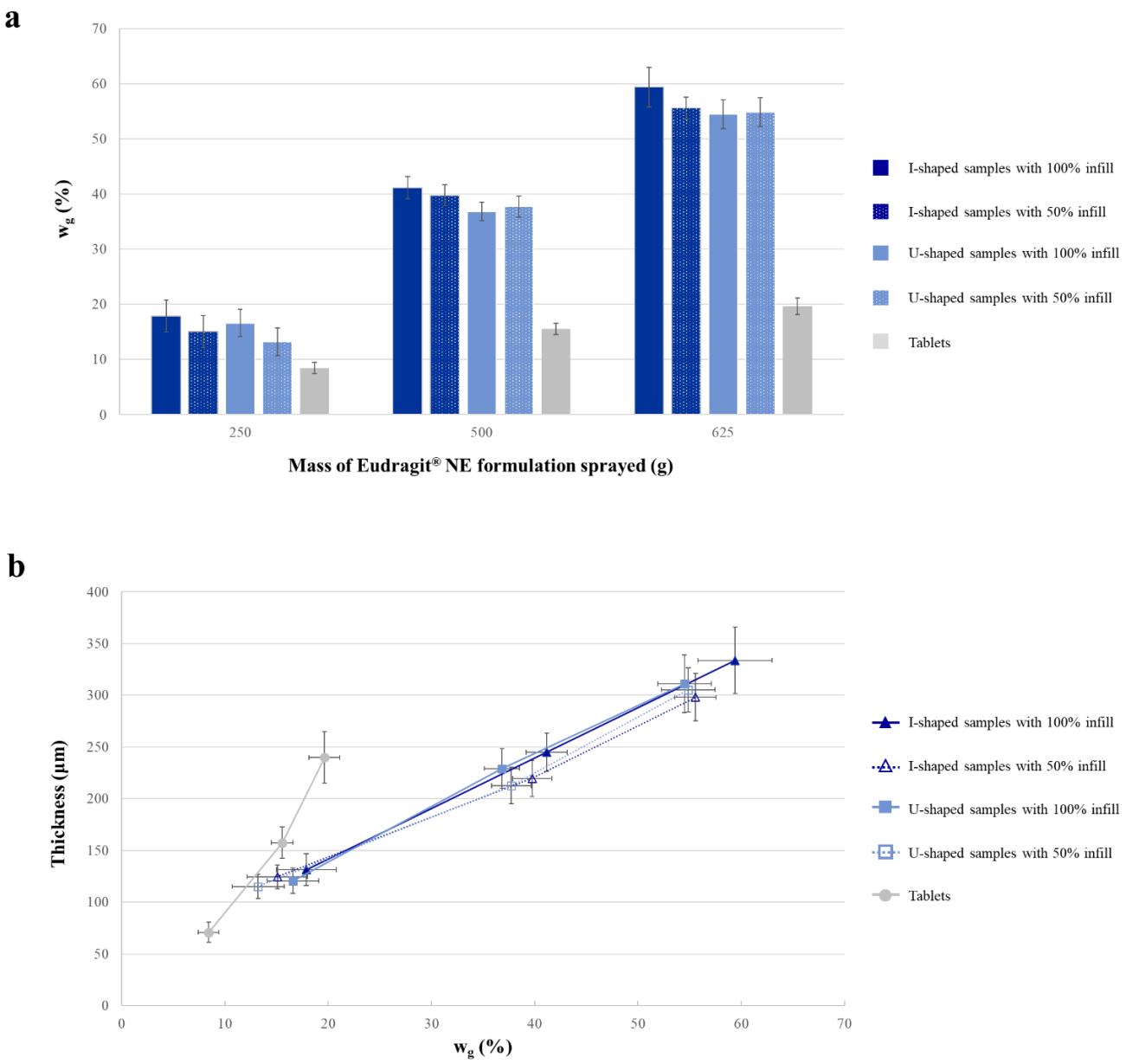

Figure 6: a) w_g and b) coating thickness data relevant to the different coated substrates (lines connecting the points in Figure b are to be intended as a guide for the eye, while the data represented are the average values attained by considering all the measurements taken from different samples and positions)

Table 5: thickness data measured on different cross-sections relevant to a) tablets as well as to b) I- and c) U-shaped samples printed with different infill

a

Mass of Eudragit® NE-based formulation sprayed (g)	Thickness, µm (CV)s	
	Tablet faces	Centre band
250	78.21 (2.63)	59.87 (6.02)
500	167.20 (5.67)	143.14 (6.57)
625	255.24 (5.90)	216.77 (7.87)

b

Mass of Eudragit® NE-based formulation sprayed (g)	Thickness, µm (CV)			
	100% infill		50% infill	
	Cross-sections		Cross-sections	
	1-4	5-6	1-4	5-6
250	139.36 (7.38)	115.53 (9.30)	129.67 (6.93)	114.69 (7.95)
500	252.21 (5.99)	230.57 (6.84)	221.94 (6.95)	215.04 (9.67)
625	343.09 (8.65)	315.04 (9.17)	305.38 (6.81)	283.55 (7.10)

c

Mass of Eudragit® NE-based formulation sprayed (g)	Thickness, µm (CV)			
	100% infill		50% infill	
	Cross-sections		Cross-sections	
	1-4	5-6	1-4	5-6
250	126.97 (6.59)	108.35 (8.34)	119.83 (7.74)	105.86 (9.81)
500	234.78 (7.30)	218.00 (8.59)	216.16 (7.30)	205.52 (9.60)
625	320.85 (7.18)	291.57 (9.53)	309.89 (5.93)	296.06 (8.47)

3.2 Coating performance

Taking into account the functionality of the 4D printed expandable DDSs under investigation, the suitability of the coating process here developed had to be confirmed, also in terms of prototypes performance, *i.e.* capability to maintain the desired shape memory effect and reproducibility of their release performance. In this respect, dealing with samples in principle intended for intravesical administration of drugs, simulated urine was employed as the medium in the following tests.

Focusing on the shape memory effect, both I- and U-shaped specimens were able to recover their original shape regardless of the presence of the coating, its thickness, and the infill percentage set during relevant 3D printing (Table 6). These results were consistent with the knowledge already acquired by testing 4D printed expandable DDSs based on PVA [13,16]. Since the systems here investigated were provided with two relatively large internal cavities, the possibility for uncoated systems of incurring in collapse/deformation phenomena during shape programming was also verified. By way of example, photographs taken during recovery experiments of I and U-shaped samples printed with 50% infill and coated with the highest amount of Eudragit® NE dispersion are reported in Figure 7. All the prototypes showed the ability to recover approximately 80% of their original shape in less than 3 min of testing. Moreover, during both programming and recovery steps, no damage to the outer film or sample collapse were highlighted. This was deemed especially promising considering that the programming of the temporary shape could only be performed after coating. Indeed, to avoid early recovery of the original shape, the samples needed to be maintained at low temperatures (*i.e.* 20 °C below their T_g), which could not be compatible with the coating process *per se*. Only minor differences were registered among specimens with diverse original shapes, but for all of them the presence of the Eudragit® NE-based external layer was confirmed to help the recovery process, reducing the time required for completing it, and increasing the relevant efficiency [13]. Indeed, the thicker the coating, the faster appeared the recovery of the original shape.

Figure 7: photographs of 50% infill samples coated with 625 g of Eudragit® NE formulation during relevant shape recovery experiment

Table 6: recovery times relevant to uncoated and coated printed samples

Mass of Eudragit® NE-based formulation sprayed (g)	I-shaped samples				U-shaped samples			
	100% infill		50% infill		100% infill		50% infill	
	$t_{RI50\%}$, s (CV)	$t_{RI80\%}$, s (CV)	$t_{RI50\%}$, s (CV)	$t_{RI80\%}$, s (CV)	$t_{RI50\%}$, s (CV)	$t_{RI80\%}$, s (CV)	$t_{RI50\%}$, s (CV)	$t_{RI80\%}$, s (CV)
0	21.67 (4.89)	47.65 (5.01)	31.00 (3.68)	175.12 (4.02)	22.08 (4.36)	49.65 (3.88)	33.51 (5.26)	162.34 (4.75)
250	23.38 (3.45)	48.37 (4.77)	34.37 (4.95)	162.34 (4.18)	24.63 (3.33)	50.11 (3.55)	20.71 (5.14)	154.86 (5.26)
500	21.89 (4.47)	40.31 (5.44)	26.27 (5.87)	97.67 (5.03)	22.58 (5.04)	38.41 (4.79)	22.21 (4.83)	98.57 (5.22)
625	18.39 (3.99)	39.43 (3.48)	25.56 (4.12)	56.36 (3.09)	23.45 (5.25)	33.46 (4.82)	22.57 (4.57)	58.90 (4.18)

The satisfactory quality of the coating process developed was further confirmed by the release performance of the coated samples. In the case of reference tablets, the resulting reservoir systems (entailing an insoluble but permeable coating based on Eudragit® NE applied onto IR cores) showed the expected prolonged release performance, with the rate of release progressively slowing down as the thickness of the applied film increased (Figure 8). The very low variability in drug diffusion through the coating was related to the overall quality and more into detail to the thickness reproducibility of the applied polymeric film.

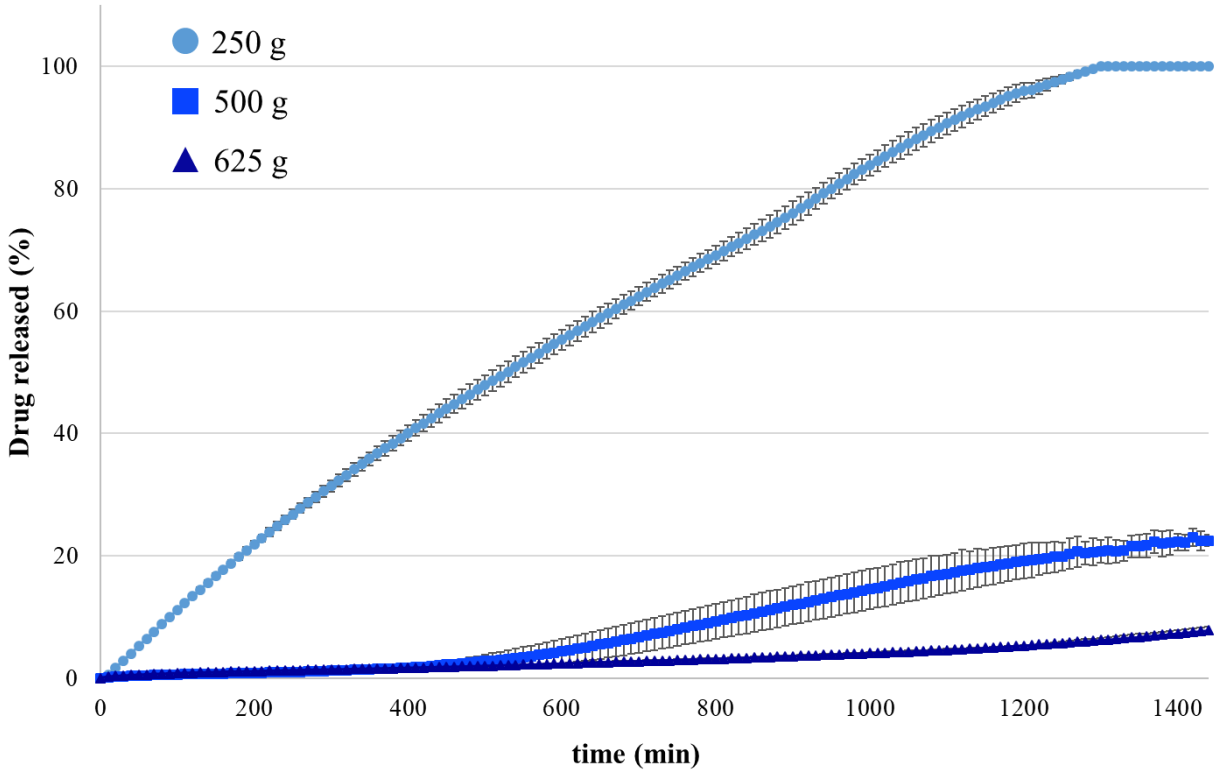

Figure 8: release profiles relevant to tables coated with different amounts of Eudragit® NE formulation

On the other hand, expandable PVA-based reservoirs pointed out a lag phase prior to the release of the conveyed drug tracer, which also turned out reproducible. Indeed, CV relevant to $t_{10\%}$ data were generally below 10% and independent from the presence of the coating film (Table 7). The release mechanism from coated expandable prototypes was previously shown to be related to the reduction

in the rate of penetration of aqueous fluids into the PVA-based matrix composing the reservoirs walls [16]. As a consequence, also the hydration, swelling and erosion/dissolution of the underlying polymer required longer times, depending on the thickness of the coating layer. Being the prototypes completely coated, the volume increase led at one point to the formation of cracks onto the external film (Figure 9). Overall, the release data obtained were in agreement with previous knowledge on the DDSs, showing the expected:

- marked increase in the $t_{10\%}$ data in the presence of the low permeable Eudragit® NE film, compared to analogous uncoated systems;
- progressively longer duration of the lag phase for specimens having thicker coatings;
- shorter lag time for the less dense systems (*i.e.* having 50% infill) when uncoated, as the rate of hydration, swelling and erosion/dissolution of the reservoirs walls increased. However, such values turned out longer when dealing with 50% infill coated specimens, due to the less efficient volume increase that deferred the formation of openings into the coating.

No obvious differences were found by comparing the behavior of I- or U-shaped samples, as the quality of the coating film was already shown independent from the specimen shape.

From the first cracking of the coating, the prototypes were unable to further restrain the release of the active ingredient contained into the cavities and a more or less rapid diffusion of drug was established. The release even lasted more than 24 h, as the complete erosion/dissolution of the PVA-based walls around the drug-containing reservoirs was hindered by the presence of a low permeable film, although discontinuous.

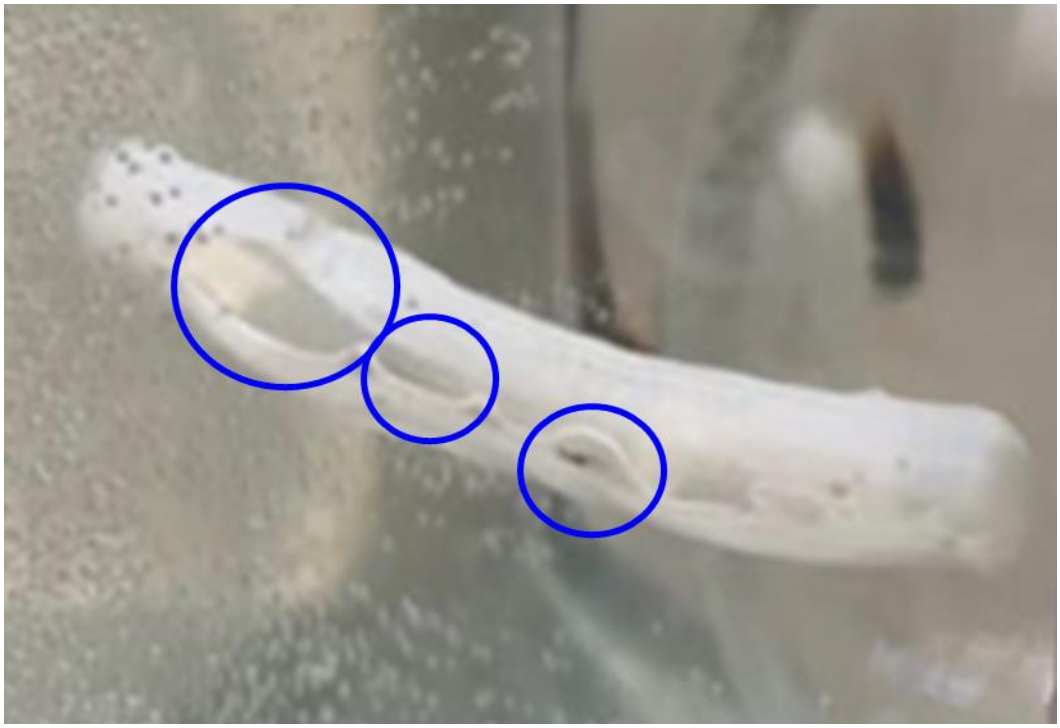

Figure 9: photograph of a coated printed samples during relevant dissolution test. Within blue circles, cracking phenomena undergone by the outer white film were highlighted. In these areas, the PVA-based material could be considered directly in contact with the dissolution medium

Table 7: release parameters relevant to different printed samples

Mass of Eudragit® NE-based formulation sprayed (g)	I-shaped samples				U-shaped samples			
	100% infill		50% infill		100% infill		50% infill	
	$t_{10\%}$, min (CV)	$t_{90\%}$, min (CV)	$t_{10\%}$, min (CV)	$t_{90\%}$, min (CV)	$t_{10\%}$, min (CV)	$t_{90\%}$, min (CV)	$t_{10\%}$, min (CV)	$t_{90\%}$, min (CV)
0	42.12 (7.93)	115.14 (8.64)	28.11 (8.36)	75.23 (9.66)	43.55 (6.99)	116.24 (9.01)	30.07 (8.37)	44.87 (10.57)
250	337.94 (8.33)	724.01 (8.12)	396.59 (6.89)	1002.26 (8.42)	325.76 (7.90)	752.00 (7.30)	371.23 (8.56)	1069.81 (9.56)
500	756.22 (6.85)	> 1440	984.55 (36.89)	> 1440	763.15 (9.48)	> 1440	975.31 (11.78)	> 1440
625	1019.59 (9.26)	> 2160	1207.38 (9.45)	> 2160	1023.45 (10.23)	> 2160	1226.36 (10.29)	> 2160

Willing to check the possibility to further slowdown the release and to modulate the load of the active ingredient conveyed into the expandable DDSs proposed, printed prototypes filled with blends of the drug tracer with either HPMC K100M or HPMC K200M and with analogous tableted formulations were finally prepared. These variants also allowed to assess the repeatability of the coating process developed using samples with different weight/apparent density with respect to those previously tested, demonstrating the possibility to attain Eudragit® NE-based coatings with the expected thickness by setting the already established process conditions. Upon contact with aqueous fluids following their diffusion through the coated walls of the systems, the HPMC-based blends were expected to promote the creation of a highly viscous gel inside the reservoir cavities. Such gel would be characterized by slow erosion/dissolution and in principle be able to further withhold the active ingredient, by entrapping it inside the system, and to slow down its diffusion once solubilized [24-27]. Starting from the same HPMC-based blends, mini-tablets of 2.5 mm in diameter were also manufactured and loaded into the printed prototypes under fabrication (*i.e.* 4 for each cavity). Besides being easy to handle, mini-tablets would ensure an accurate dosing and could also represent an advantageous strategy for improving the overall drug content.

The coating process of U-shaped prototypes printed with 100% infill and containing these new formulations was carried out up to the first w_g already described (*i.e.* 250 g of Eudragit® NE-based formulation sprayed). It allowed to achieve quite similar coating films in the range of 125-138 µm, regardless of the type of filling conveyed within the prototype cavities. All the coated samples pointed out a good reproducibility in terms of weight (1110.36 mg, CV = 7.11 and 1142.10 mg, CV = 8.43 for HPMC K100M-based powder blend and mini-tables; 1237.94 mg CV = 6.93 and 1177.43 mg, CV = 7.52 for HPMC K200M-based powder blend and mini-tables). Moreover, the release performance of the coated specimens turned out consistent with the above-mentioned operating hypothesis (Table 8). Notably, for both powder and tablet-filled specimens, those containing the HPMC with the highest molecular weight (*i.e.* HPMC K200M) exhibited the longest $t_{10\%}$ and $t_{90\%}$ values. With respect to the uncoated prototypes tested for reference purposes, the behavior of samples

filled with mini-tablets was impaired by the leakage of the latter once the cavities opened. This is the reason why $t_{90\%}$ data should not be considered relevant, because they would be associated to the matrix nature of the tablets and not to the overall capability of the whole device to control drug release.

Focusing on the shape recovery behavior, the expandable DDSs filled with the new formulations based on the high molecular weight HPMC K100M and K200M were deemed particularly critical in view of their expected swelling. In addition, the presence of tablets, being solid units, could determine a certain stiffness of the printed specimens, thus challenging both the programming of the temporary configuration and the recovery of the original one. Interestingly, no issues were faced in both the above-mentioned steps, thus confirming the possibility of varying the filling without compromising the operating mechanism of the PVA-based organ-retentive prototypes under development.

Table 8: release parameters relevant to U-shaped samples printed with 100% infill and filled with drug containing powder blends or mini-tablets based on either HPMC K100M or HPMC K200M

		Mass of Eudragit® NE-based formulation sprayed (g)			
		0		**250**	
		$t_{10\%}$, min (CV)	**$t_{90\%}$, min (CV)**	**$t_{10\%}$, min (CV)**	**$t_{90\%}$, min (CV)**
HPMC K100M-based	powder blend	75.40 (13.81)	197.37 (16.0)	407.35 (10.23)	> 1440
	mini-tablets	83.17 (5.27)	546.94 (2.67)	473.69 (7.78)	> 2160
HPMC K200M-based	powder blend	99.21 (14.69)	220.79 (25.69)	527.45 (12.34)	> 1440
	mini-tablets	96.89 (19.30)	570.40 (14.26)	515.39 (9.46)	> 2160

4. Conclusions

The present work represents a major step forward in assessing the potential of PVA-based expandable DDSs targeting long-lasting retention and prolonged release into hollow muscular organs such as the

bladder. Indeed, 4D printed prototypes were successfully coated with an insoluble and poorly-permeable film based on Eudragit® NE, despite the possible challenges entailed by their complex (*i.e.* either elongated or folded) shapes. The coating process was shown reproducible, leading to the achievement of samples with good physical properties and technological features, such as reproducible coating thickness, consistent release performance and capability to effectively undertake the shape shifting involved by programming of the temporary shape as well as recovery, following interaction with aqueous fluids at body temperature, of the original one. In addition, the quality of the coating applied was shown independent of the geometry (*i.e.* I and U shapes) and apparent density of the samples considered, of the presence of internal cavities as well as of relevant filling. Resorting to an equipment configured for pilot/industrial production, the adjustments implemented and the operating conditions selected would be useful in view of further scale-up of the retentive DDSs under investigation. Indeed, the results attained by processing screening samples of such critical shapes, composition and expected working mechanism as well as performance would be promising in terms of chances to overcome the challenges related to industrial-level coating of new and more advanced prototypes.

References

1. Melocchi A., Inverardi N., Uboldi M., Baldi F., Maroni A. Pandini S., Briatico-Vangosa F., Zema L., Gazzaniga A, 2019, Retentive device for intravesical drug delivery based on water-induced shape memory response of poly(vinyl alcohol): design concept and 4D printing feasibility, Int. J. Pharm. 559: 299-311
2. Melocchi A., Uboldi M., Inverardi N., Briatico-Vangosa F., Baldi F., Pandini S., Scalet G., Auricchio F., Cerea M., Foppoli A., Maroni A., Zema L., Gazzaniga A., 2019, Expandable drug delivery system for gastric retention based on shape memory polymers: Development via 4D printing and extrusion. Int. J. Pharm., 571: 118700
3. Inverardi N., Scalet G., Melocchi A., Uboldi M., Maroni A., Zema L., Gazzaniga A., Auricchio F., Briatico-Vangosa F., Baldi F., Pandini S., 2021, Experimental and computational analysis of a pharmaceutical-grade shape memory polymer applied to the development of gastroretentive drug delivery systems, J. Mech. Behav. Biomed Mater., 124: 104814
4. Dhiman S., Philip N., Singh T.G., Babbar R., Garg N., Diwan V., Singh P., 2023, An Insight on Novel Approaches & Perspectives for Gastro-Retentive Drug Delivery Systems, Current Drug Deliv., 20: 708-729
5. Mahmoud D.B., Schulz-Siegmund M., 2023, Utilizing 4D printing to design smart gastroretentive, esophageal, and intravesical drug delivery systems, Adv. Healthc. Mater., 12: 2202631
6. Palugan L., Cerea M., Cirilli M., Moutaharrik A., Maroni A., Zema L., Melocchi A., Uboldi M., Filippin I., Foppoli A., Gazzaniga A., 2021, Intravesical drug delivery approaches for improved therapy of urinary bladder diseases, Int. J. Pharm. X, 3: 100100
7. Vrettos N.-N., Roberts C.J., Zhu Z., 2021, Gastroretentive technologies in tandem with controlled-release strategies: A potent answer to oral drug bioavailability and patient compliance implications, Pharmaceutics, 13: 1591

8. Gazzaniga A., Foppoli A., Cerea M., Palugan L., Cirilli M., Moutaharrik S., Melocchi A., Maroni A., 2023, Towards 4D printing in pharmaceutics, Int. Journal Pharm. X, 5: 100171
9. Melocchi A., Uboldi M., Cerea M., Foppoli A., Maroni A., Moutaharrik S., Palugan L., Zema L., Gazzaniga A., 2021, Shape memory materials and 4D printing in pharmaceutics, Adv. Drug Deliv. Review, 173: 216-237
10. Singh Sharma K., 2023, Artificial intelligence assisted fabrication of 3D, 4D and 5D printed formulations or devices for drug delivery, Current Drug Deliv. 20: 752-769
11. Maroni A., Melocchi A., Zema L., Foppoli A., Gazzaniga A, 2020, Retentive drug delivery systems based on shape memory materials, J. Appl. Polym. Sci., 137: 48798
12. Uboldi M., Melocchi A., Moutaharrik S., Palugan L., Cerea M., Foppoli A., Maroni A., Gazzaniga A., Zema L., 2022, Administration strategies and smart devices for drug release in specific sites of the upper GI tract, J. Control. Release, 348: 537-552
13. Uboldi M., Pasini C., Pandini S., Baldi F., Briatico-Vangosa F., Inverardi N., Maroni A., Moutaharrik S., Melocchi A., Gazzaniga A., Zema L., 2022, Expandable drug delivery systems based on shape memory polymers: impact of film coating on mechanical properties and release and recovery performance, Pharmaceutics, 14: 2814
14. Melocchi A., Parietti F., Maroni A., Foppoli A., Gazzaniga A., Zema L., 2016, Hot-melt extruded filaments based on pharmaceutical grade polymers for 3D printing by fused deposition modeling, Int. J. Pharm., 509: 255-263
15. Patra C.N., Priya R., Swain S., Kumar Jena G., Panigrahi K.C., Ghose D., 2017, Pharmaceutical significance of Eudragit: A review, Future J. Pharm. Sci., 3: 33-45
16. Uboldi M., Perrotta C., Moscheni C., Zecchini S., Napoli A., Castiglioni C., Gazzaniga A., Melocchi A., Zema L., 2023, Insights into the safety and versatility of 4d printed intravesical drug delivery systems, Pharmaceutics, 15: 757
17. Sherif A.Y., Mahrou G.M., Alanazi F.K., 2018, Novel in-situ gel for intravesical administration of ketorolac, Saudi Pharm. J. 26: 845-851

18. Melocchi A., Uboldi M., Briatico-Vangosa F., Moutaharrik S., Cerea M., Foppoli A., Maroni A., Palugan L., Zema L., Gazzaniga A., 2021b, The Chronotopic™ system for pulsatile and colonic delivery of active molecules in the era of precision medicine: Feasibility by 3D printing via fused deposition modeling (FDM), Pharmaceutics, 13: 759
19. Pandey P., Turton R., Joshi N., Hammerman E., Ergun J., 2006, Scale-up of a pan-coating process, AAPS PharmSciTech., 7: 102
20. Uboldi M., Melocchi A., Moutaharrik S., Cerea M., Gazzaniga A., Zema L., 2021, Dataset on a small-scale film-coating process developed for self-expanding 4D printed drug delivery devices, Coatings, 11: 1252
21. Freireich B., Ketterhagen W.R., Wassgren C., 2011, Intra-tablet coating variability for several pharmaceutical tablet shapes, Chem. Eng. Sci., 66(12): 2535-2544
22. Wahl P.R., Peter A., Wolfgang M., Khinast J.G., 2019, How to measure coating thickness of tablets: Method comparison of optical coherence tomography, near-infrared spectroscopy and weight-, height- and diameter gain, Eur. J. Pharm. Biopharm., 142: 344-352
23. Brock D., Zeitler J.A., Funke A., Knop K., Kleinebudde P., 2013, Evaluation of critical process parameters for intra-tablet coating uniformity using terahertz pulsed imaging, Eur. J. Pharm. Biopharm., 85(3): 1122-1129
24. Alderman D.A., 1984, A review of cellulose ether in hydrophilic matrices for oral controlled release dosage forms, Int. J. Pharm. Tech. Prod. Mfr., 5: 1-9
25. Jamzad S., Tutunyi L., Fassihi R., 2005, Analysis of macromolecular changes and drug release from hydrophilic matrix systems, Int. J. Pharm., 292: 75-85
26. Melia C.D., 1991, Hydrophilic matrix sustained release systems based on polysaccharide carriers, Crit. Rev. Ther. Drug Carrier Syst., 8: 395-421
27. Varma M.V.S., Kaushal A.M., Garg A., Garg S., 2004, Factors affecting mechanism and kinetics of drug release from matrix based oral controlled drug delivery systems, Am. J. Drug Deliv., 2: 43-57

Graphical Abstract

Click here to access/download;Graphical Abstract;Uboldi M. et al., Graphical abstract.jpg

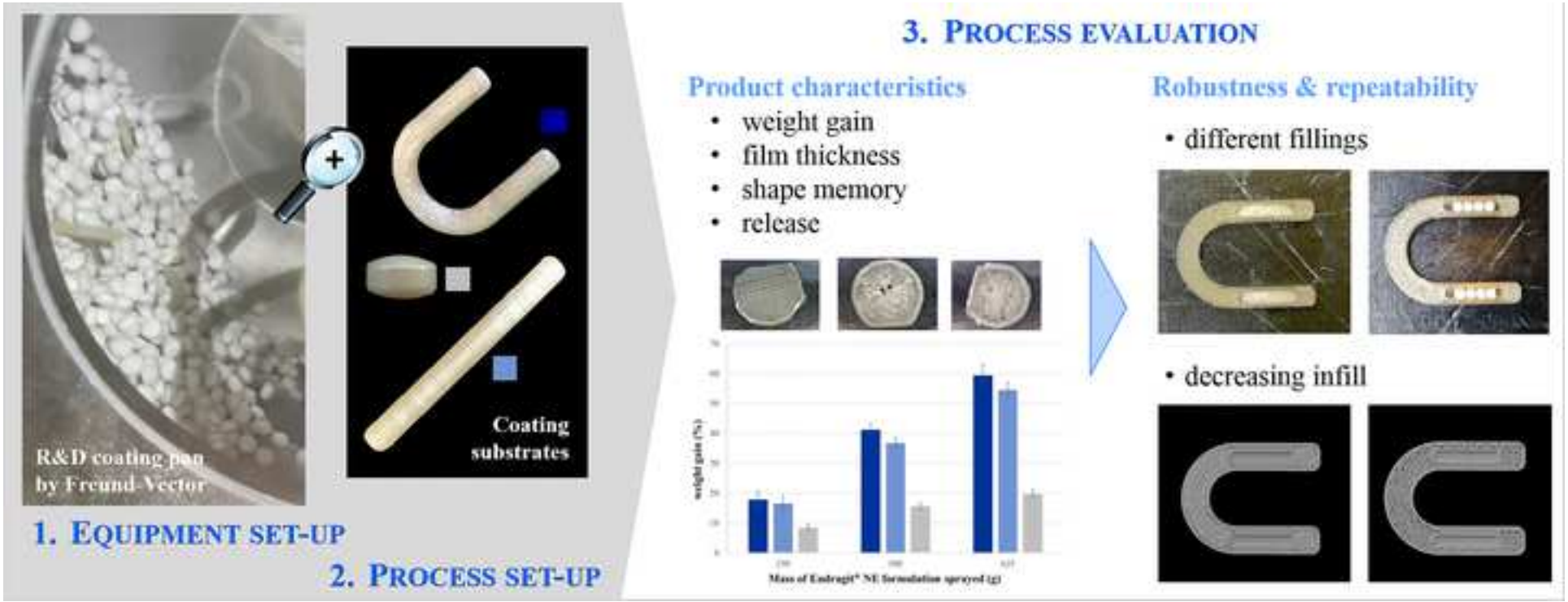

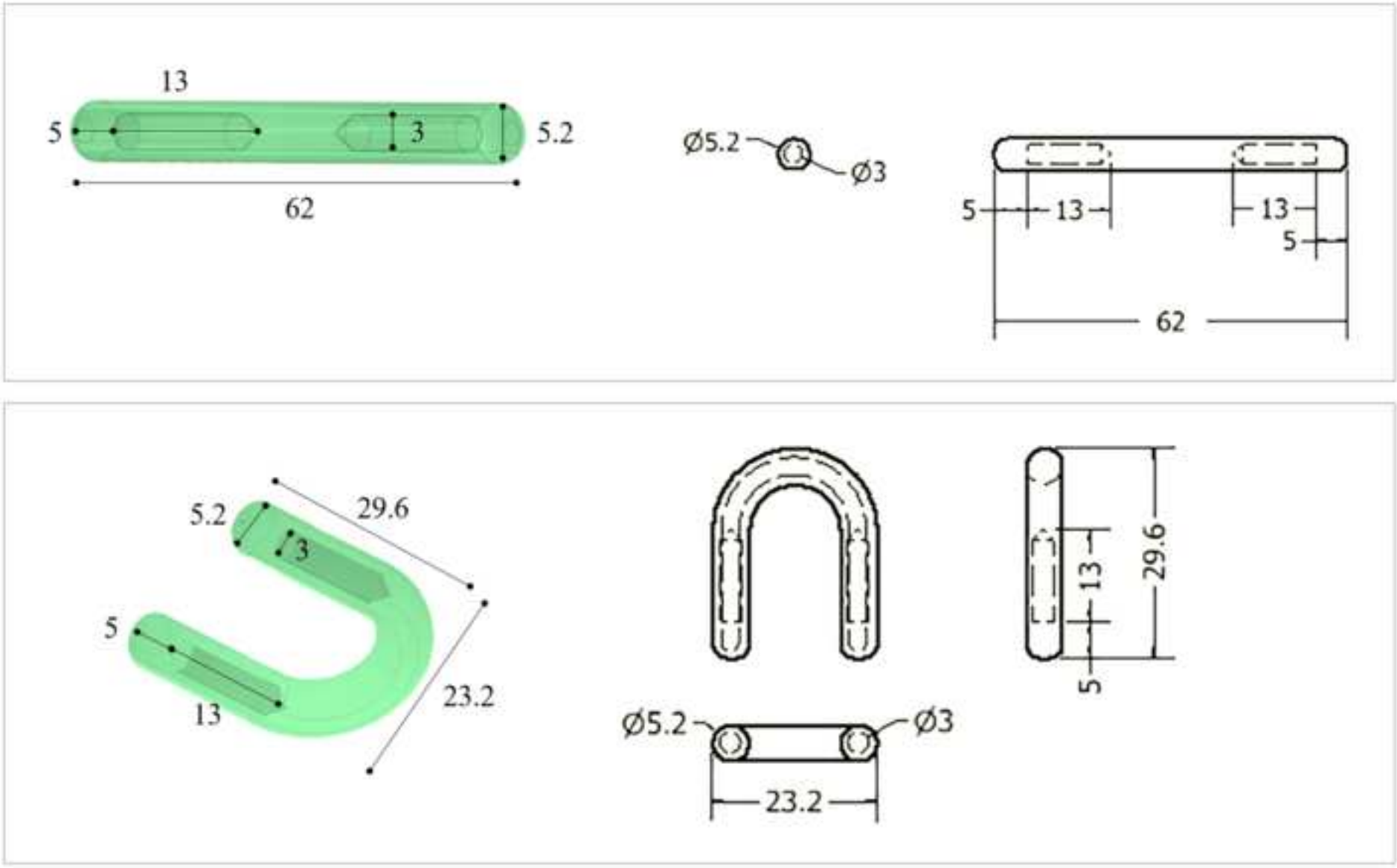

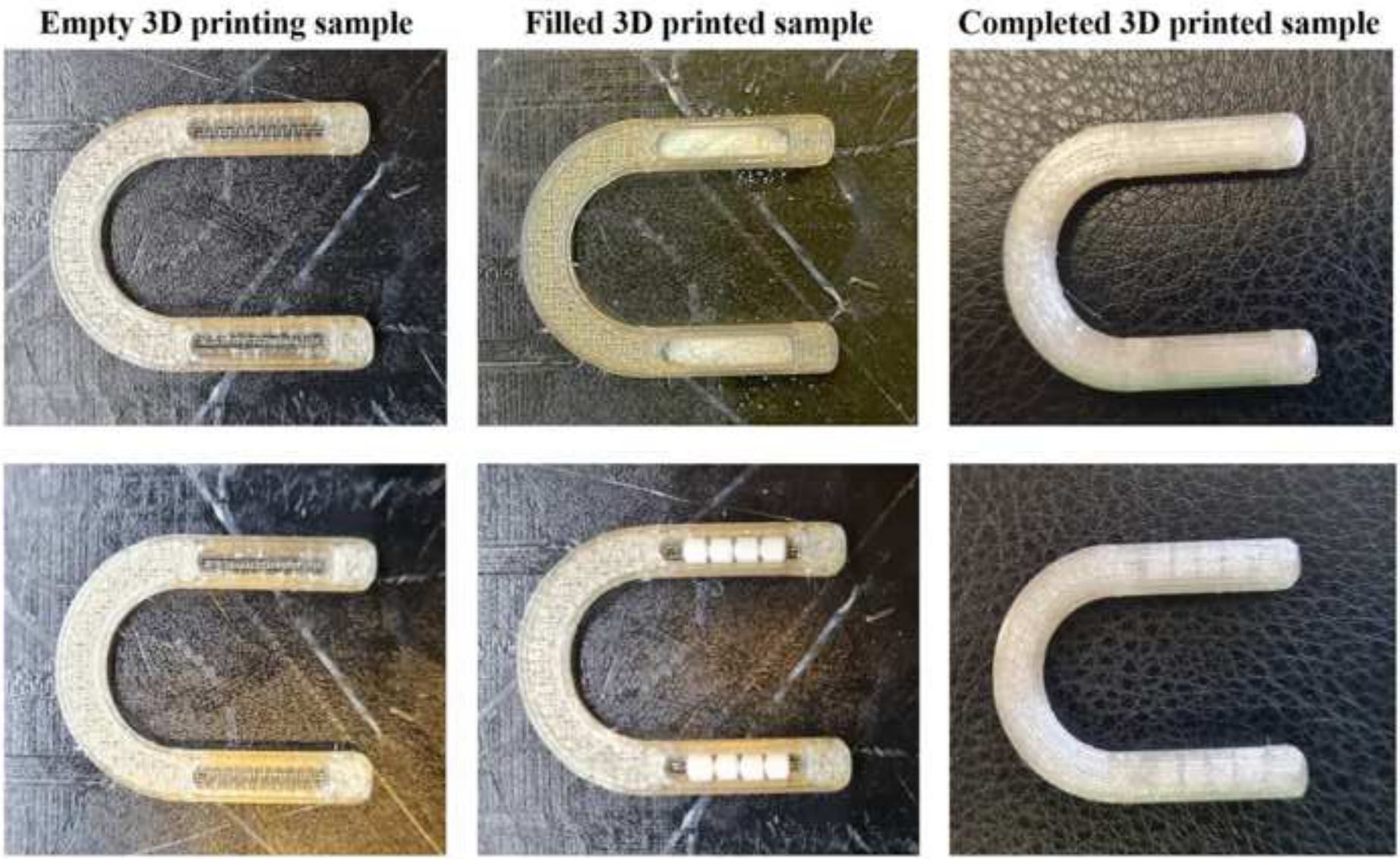

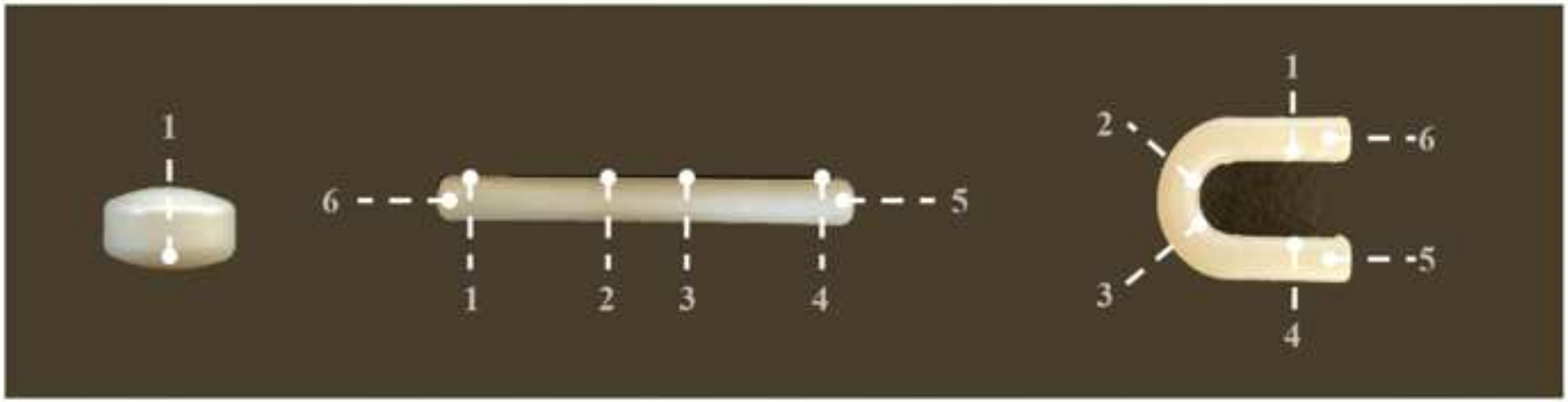

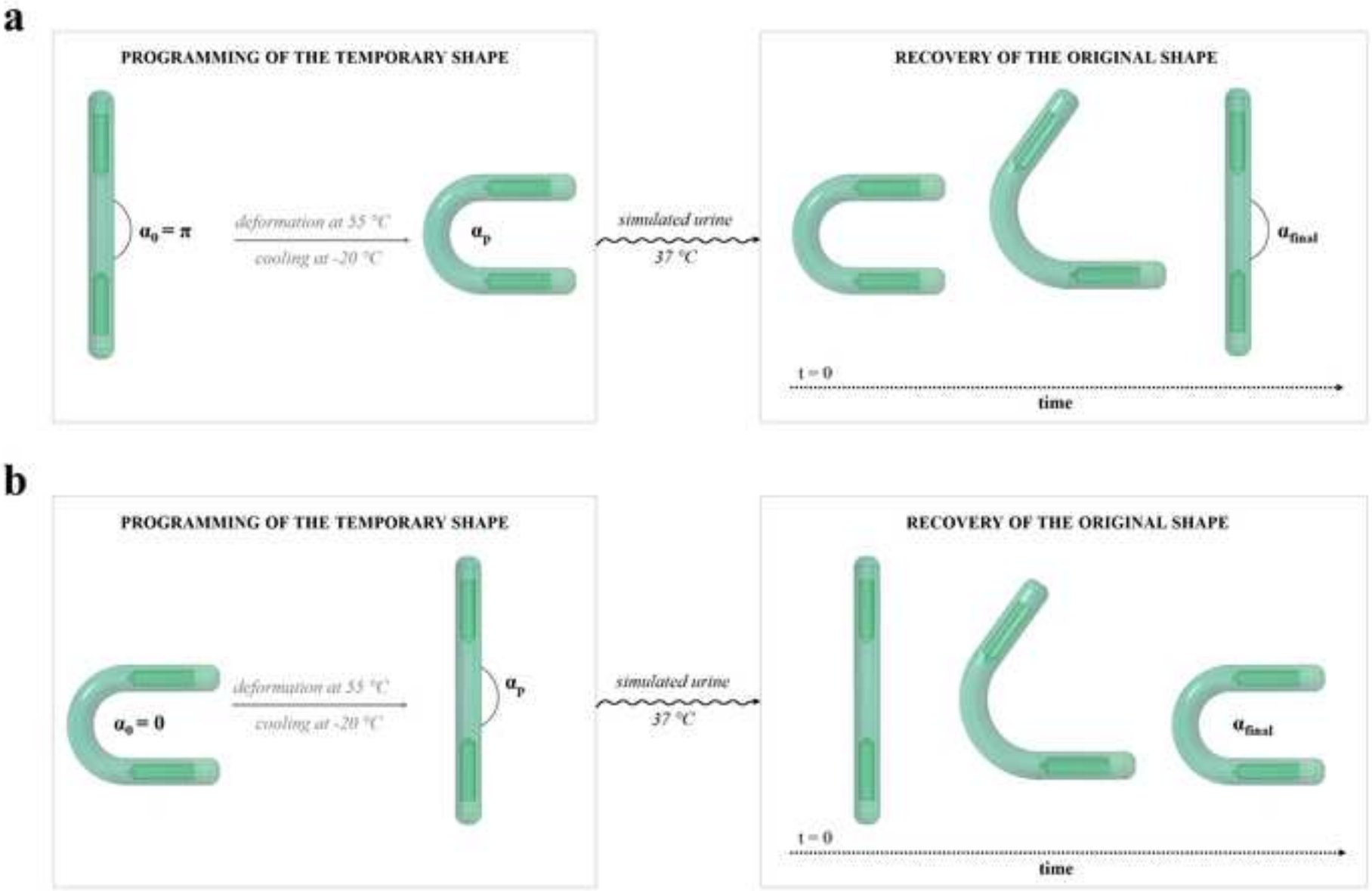

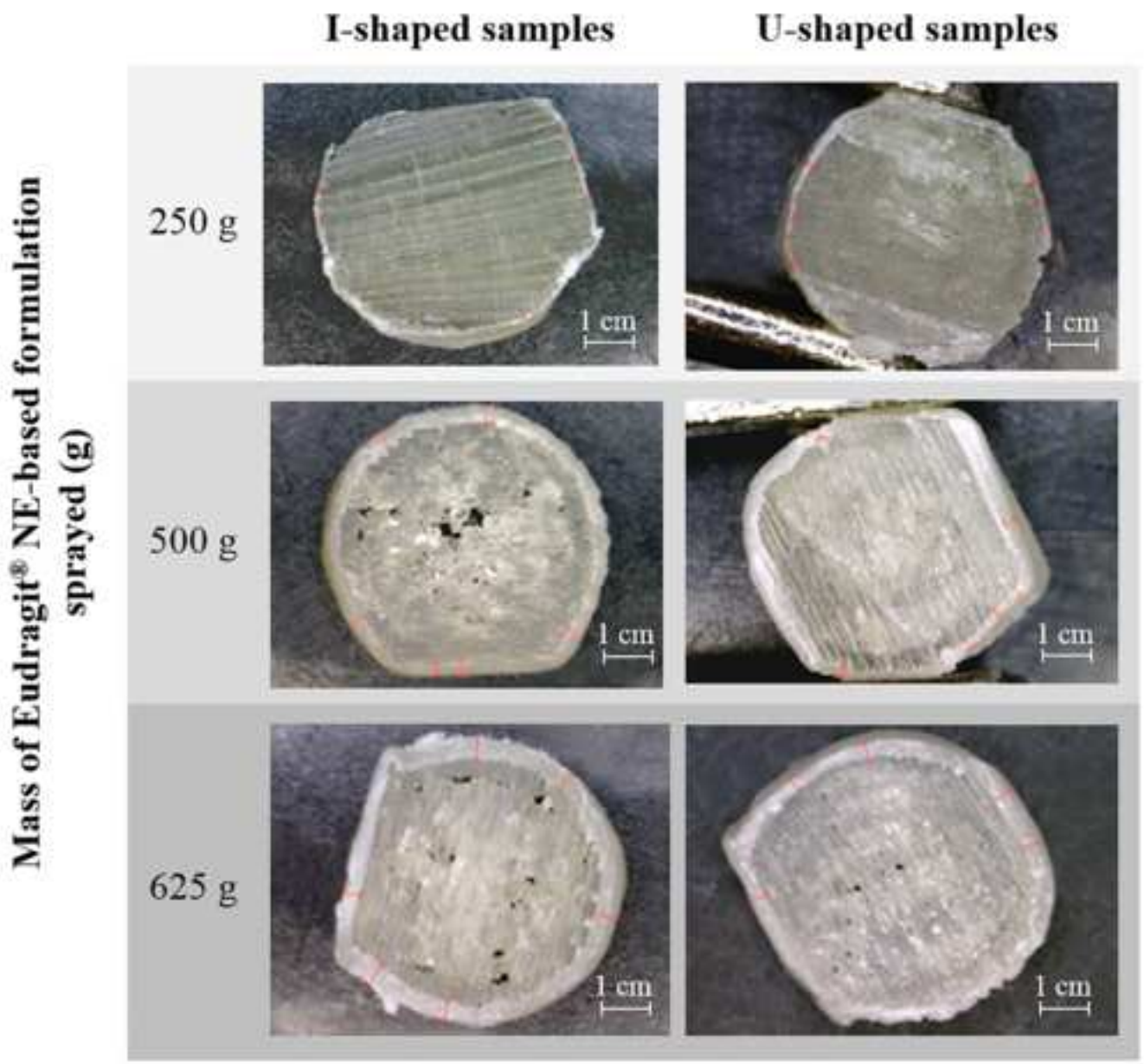

Figure 6 revised

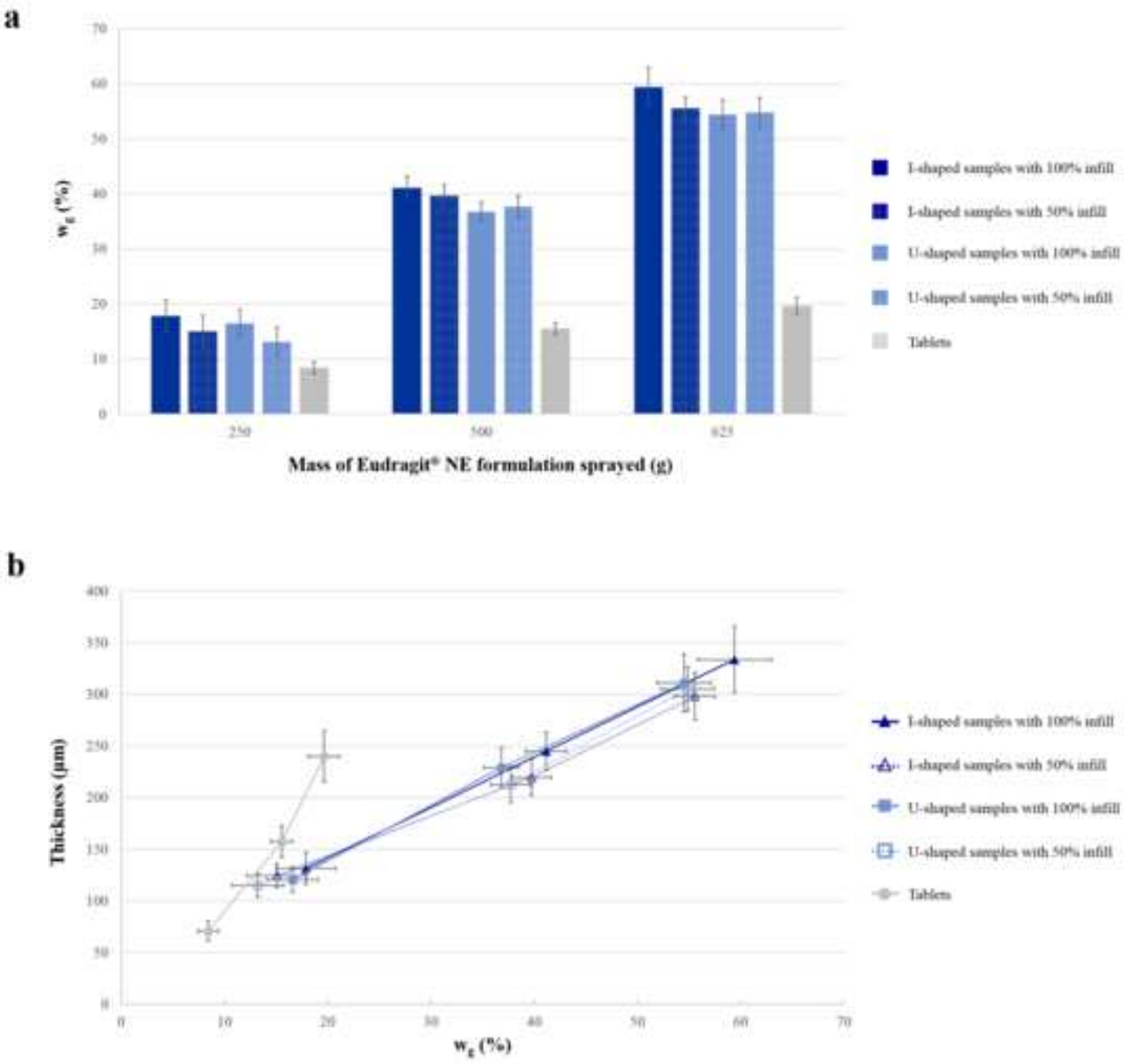

Figure 8 revised

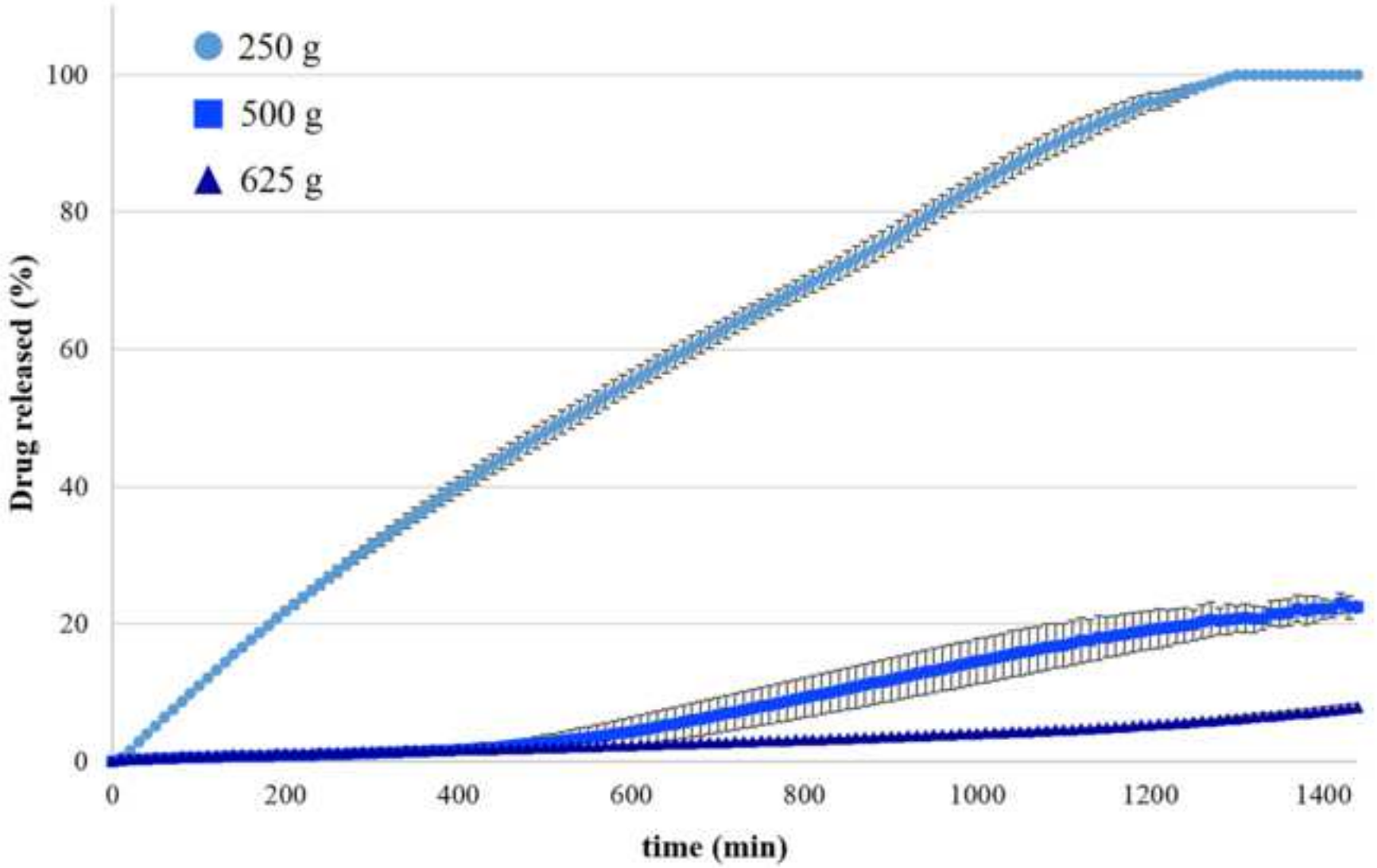

Figure 9 revised

Click here to access/download;Figure;Uboldi M. et al., Figure 9 revised.tif

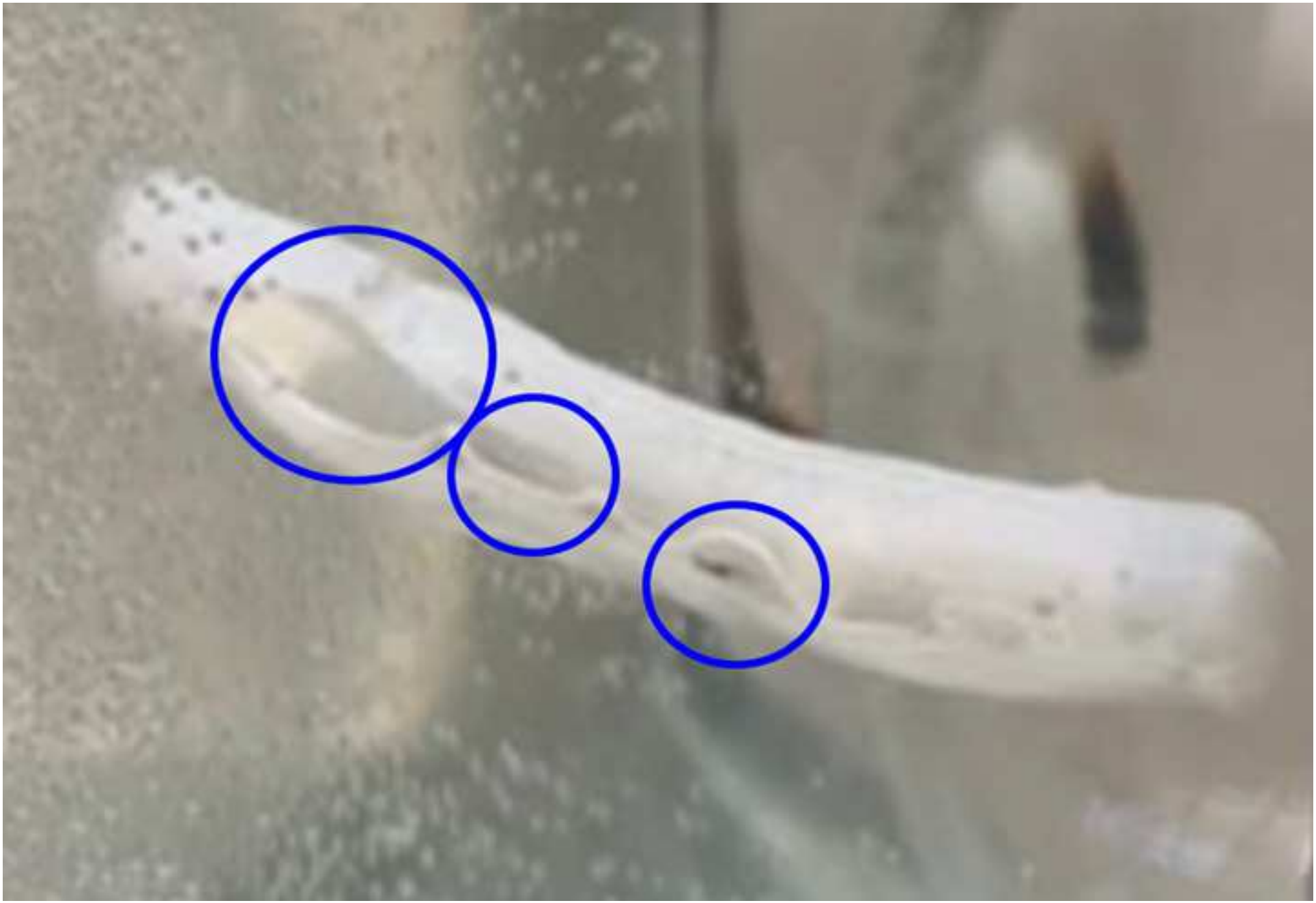

Declaration of interests

☐ The authors declare that they have no known competing financial interests or personal relationships that could have appeared to influence the work reported in this paper.

☒The authors declare the following financial interests/personal relationships which may be considered as potential competing interests:

We wish to draw the attention of the Editor to the following:

- the coating pan employed in this study was modified by Freund-Vector Corporation;
- G. Buratti and A. Gelain wish to disclose that they work for the European lab of Freund-Vector Corporation.

We would like to confirm that there has been no financial support for this work that could have influenced its outcome and Freund-Vector did not provide any funding for the present scientific study.

Marco Uboldi: Data Curation, Investigation, Writing - Original Draft, Conceptualization

Andrea Gelain: Data Curation, Investigation, Writing - Original Draft

Giuseppe Buratti: Resources, Methodology, Writing - Review & Editing

Andrea Gazzaniga: Writing - Review & Editing, Conceptualization, Resources

Alice Melocchi: Conceptualization, Methodology, Project administration, Writing - Original Draft, Writing - Review & Editing

Lucia Zema: Conceptualization, Supervision, Writing - Review & Editing, Resources